CHAPTER IV

SYNTHESIS OF MCM-41 FROM RICE HUSK SILICA

4.1 Introduction

Due to the fact that rice husk ash is a cheap source of an active form of hydrated amorphous silica, it has been utilized in various material applications. The synthesis of microporous materials such as zeolites from rice husk silica has been introduced [Hamdan, 1997; Wang, 1998; Lohsoontorn, 2002]. It has been investigated that the zeolites obtained from rice husk silica perform with high crystallinity and uniform pore size distribution similar to that of commercial silica. Nowadays, these synthetic zeolites have been widely used for catalytic applications. The success in zeolite prepared from rice husk silica has motivated us to pay more attention in the synthesis of other molecular sieve materials. MCM-41, a mesoporous material with a uniform pore diameter in the range of 20-500 Å, well-defined hexagonal shape and narrow pore size distribution is very attractive in environmental applications, such as adsorption and catalytic reaction. Unfortunately, the MCM-41 material has not been commercialized so far. Either sodium silicate or fumed silica used as a reactant for the classical MCM-41 synthesis is obtained from quartz. The high cost in the process of changing the crystallinity phase of quartz to a reactive silica results in an expensive commercial MCM-41 product. In stead of using commercial silica, silica extracted from rice husk obtained from Chapter II is extremely attractive.

In this chapter, an alternative challenge in waste management is proposed. The effort is focused on the utilization of rice husk silica as a raw material for the synthesis of mesoporous catalyst support, which can be applied to chlorinated adsorption and its hydrodechlorination of volatile organic compounds.

4.2 Objectives

With the corporation of a waste utilization program, this chapter aims to add to the value adding of rice husk silica by using it as a replacement of commercial silica in the synthesis of MCM-41. The preliminary application of RH-MCM-41 was conducted by the adsorption of some chlorinated volatile organic compounds (CVOCs), compared with the commercial adsorbents. The specific purposes are as follows:

1. To utilize the extracted rice husk silica from Chapter II for MCM-41 synthesis.
2. To study the influences of synthesis parameters such as aging time and pH values on the crystallinity of the final product MCM-41.
3. To examine the physical characteristics and chemical compositions of MCM-41 synthesized from rice husk silica (RH-MCM-41) and compare them with the parent MCM-41 obtained from the previous chapter.
4. To determined the capacity and behavior of CVOCs adsorption on RH-MCM-41 compared with the mordenite and activated carbon.

4.3 Experimental

Materials and apparatus used for the synthesis of MCM-41 from extracted rice husk silica in this chapter were set up by following the procedures in Chapter III. To understand the significant parameters related to the formation of a liquid crystal in the early stage of the MCM-41 synthesis, the studied parameters of pH and aging time are reported.

4.3.1 Methodology

The synthesis of RH-MCM-41 mostly followed the procedure described for a parent MCM-41 in Chapter II. CTAB was still used as a template. However, TEOS was replaced by our sodium silicate solution, which was prepared from a mixture of sodium hydroxide and rice husk silica obtained in Chapter II. The molar compositions of the gel were $1SiO_2 : 1.09NaOH : 0.13CTAB : 0.12H_2O$. The synthesis procedures are listed consequently as follows:

1. Sodium hydroxide solution was initially prepared by dissolving 0.38 g of sodium hydroxide in 50 mL of deionized water contained in a Teflon beaker.
2. 1 g of CTAB was then transferred to that alkali solution and vigorously stirred until the solution was homogeneous.
3. Sodium silicate was prepared in another container by dissolving 0.672 g of sodium hydroxide in 2.69 mL of deionized water. Then, 1.44 g of rice husk silica was added and the solution was heated gently until it was clear and viscous.
4. After that the CTAB alkali solution was poured into a sodium silicate container. The mixture was mechanically stirred for 30 minutes without the synthesis pH control. Then, the gel was continuously stirred at room temperature for aging. To study the effect of aging time on the crystallinity change, the aging time was varied from 24, 36, 48 and 60 h. The optimum aging time that provided the high intensity of XRD patterns in the *d100* crystallinity peak was selected for the study of pH effect in the same

manner. The desired pH values were studied from 9, 10 and 11 by adjustment with 1% HCl. .

5. After aging, the suspended solid was filtered through Whatman paper with sieve size No. 48 and washed with ethanol and finally rinsed with deionized water before calcination in the furnace at 550 °C for 5 h under airflow.

4.3.2 Sample Characterizations

Similar to the characterizations of the parent MCM-41 discussed previously in Chapter III, the physical characteristics and chemical compositions of RH-MCM-41 were examined by the same techniques. The formation of crystallinity was studied by XRD diffraction. Porous characteristics of the sample such as specific surface area, pore diameter, pore volume and pore size distribution were determined by nitrogen adsorption isotherm combined with BET method. The functional groups within MCM-41 were examined by FTIR spectroscopy. The physical morphologies were observed by SEM and TEM microscopic techniques.

4.3.3 Results and Discussion

4.3.3.1 XRD Characteristics

The XRD diffractograms of RH-MCM-41 prepared at room temperature and the aging time ranging from 24-60 h without synthesis pH control are shown in Figure 4-1. Similar to the XRD patterns of the parent MCM-41, the XRD of RH-MCM-41 exhibited four pronounced peaks indicating a high structural ordering of the MCM-41 materials corresponding to Bragg peaks in the range of 2θ between 2-8 at 2.6, 4.2, 4.8, and 6.0 which are representative of the most syntheses of pure silica MCM-41 reported elsewhere [Beck, 1992; Chen, 1993; Ciesla, 1999]. It was noticed that within 24 h after all reactants were mixed and the pH value of the mixture was adjusted to 10, an initial precipitate was formed by the assumption of self-assembled tubular

mesostructures exhibited at a *hkl* reflection equal to *d100*. Other identical peaks such in *d110, d200* and *d210* were observed when the aging time increased. The XRD spectrum of 60 h aging time shows the most complete orientation of tubular structures. However, it was seen that precipitation within 48 h was adequate for stabilization of ordered mesoporous molecular sieves.

Figure 4-2 shows comparisons of the XRD patterns of assynthesized RH-MCM-41 and calcined RH-MCM-41 of which the synthesis pH were varied from 9-11 and the aging time was 48 h. The differences in pH led to the changes in the XRD crystallinity of calcined samples. When the pH value less or more than 10, the intensity of *d100* peak was obviously lower as well as other reflection peaks. On the other hand, well-ordered RH-MCM-41 was obtained from the synthesis mixture of which the optimized pH was adjusted at 10. It was indicated that without the synthesis pH adjustment, the well-defined porous structures of MCM-41 were not satisfactorily obtained. These results can be explained by a lower degree of polycondensation of the silicate species when the pH value of the gel is too high or too low. This results in the greater contraction of the pores and the tendency of disordered assembly after calcination [Voegtlin et al., 1997]. The broad peak at *d100* of an uncalcined sample is caused by the low stability of the lamellar phase structure. Upon calcination at 550 °C for 5 h, the rod like silicate complex is reorganized and the pore structure is eventually contracted to form a more stable hexagonal mesoporous material, which attributes to an increase of the intensity of the XRD peaks by about 2.5 times and the resolution of the higher order peaks. RH-MCM-41, which provided the best quality of XRD crystalline results, was selected as the representative sample used for other characterizations mentioned later and prepared for the catalyst support in Chapter V.

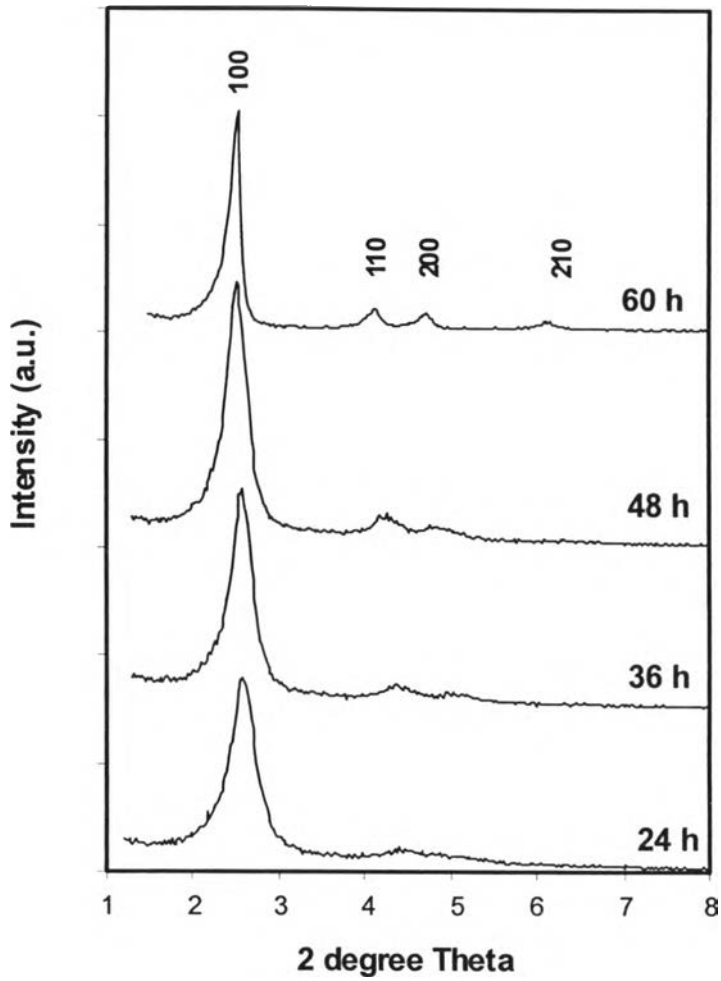

Figure 4-1 X–ray powder diffraction patterns of RH-MCM-41 at various aging time from 24 to 60 h and at a pH value of 11.

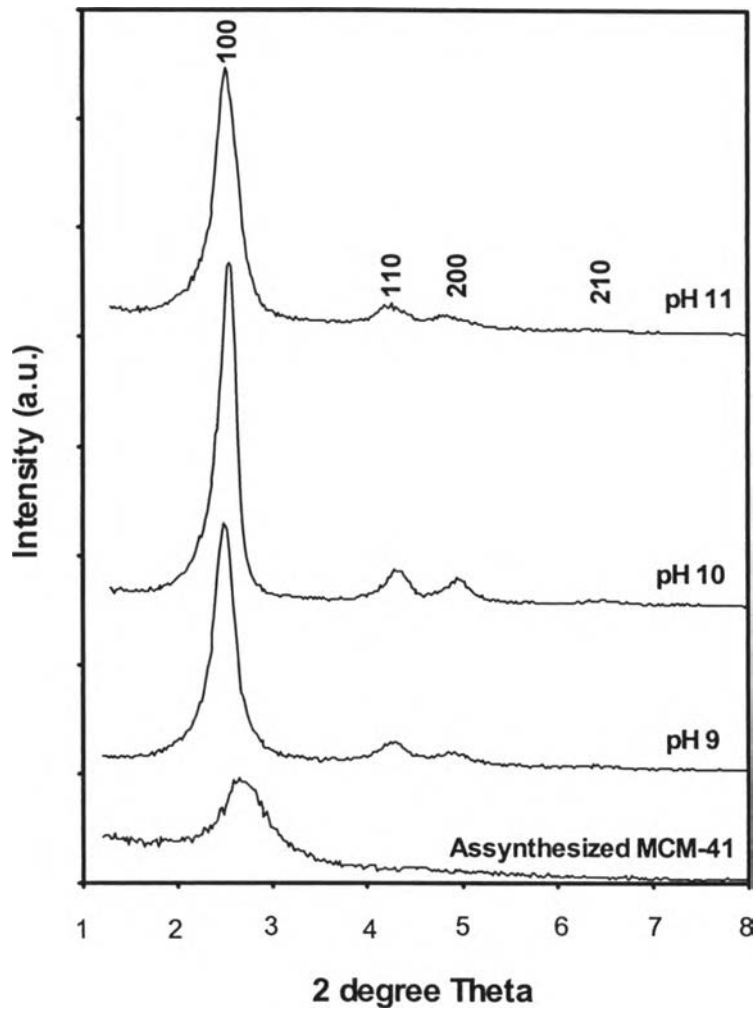

Figure 4-2 X–ray powder diffraction patterns of assynthesized and calcined RH-MCM-41; synthesized at an aging time of 48 h with various pH values from 9 to 11.

4.3.3.2 Nitrogen Adsorption Isotherm and BET Analysis

The nitrogen adsorption isotherm for RH-MCM-41 particles is shown in Figure 4-3. According to the new classification, the isotherm was Type IVc, which is the same type of isotherm as the parent MCM-41. As the relative pressure increases, the isotherms exhibit sharp inflection, which is the characteristic of capillary condensation within uniform mesopores. The ratio P/P_0 at the inflection point is related to the diameter of the mesopores. The capillary condensation in a very narrow range $0.2<P/P_0<0.3$ demonstrated that the RH-

MCM-41 particles have nearly uniform pore size. The total surface area of the RH-MCM-41 particles evaluated by using the BET theory was (800 ± 80) $m^2 g^{-1}$. The pore size distribution from the nitrogen isotherm produced by using the BJH is shown in Figure 4-4. The BJH pore size distribution curves shows the MCM particles with quite a narrow pore diameter distribution, which is centered at 29.0 Å with a pore volume of 0.93 $cm^{-3} g^{-1}$.

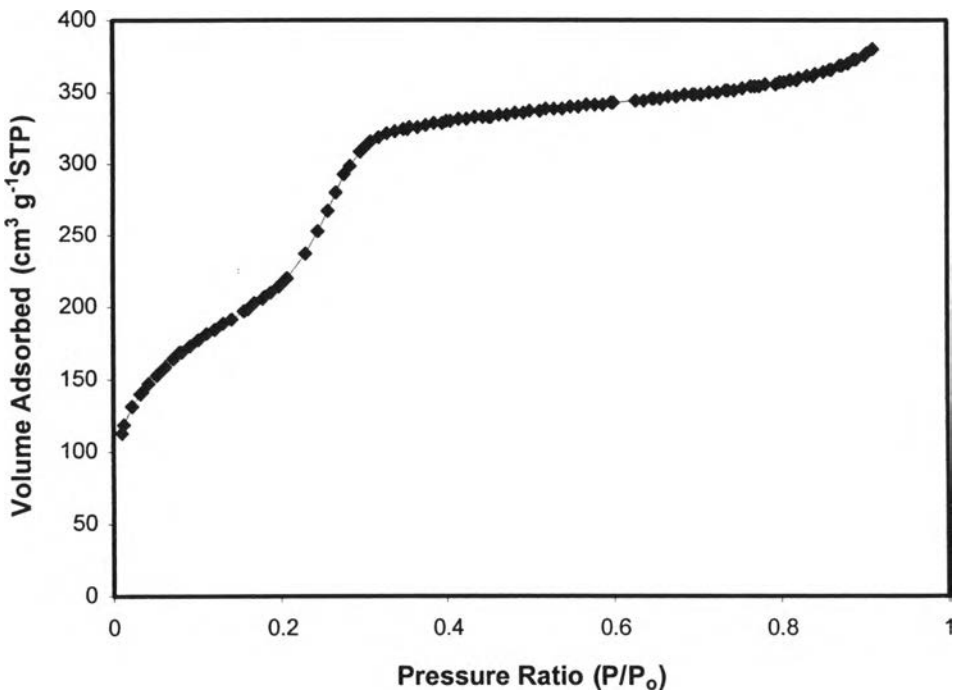

Figure 4-3 Adsorption isotherm of nitrogen gas at 77 K for RH-MCM-41 at an aging time of 48 h and pH value of 10.

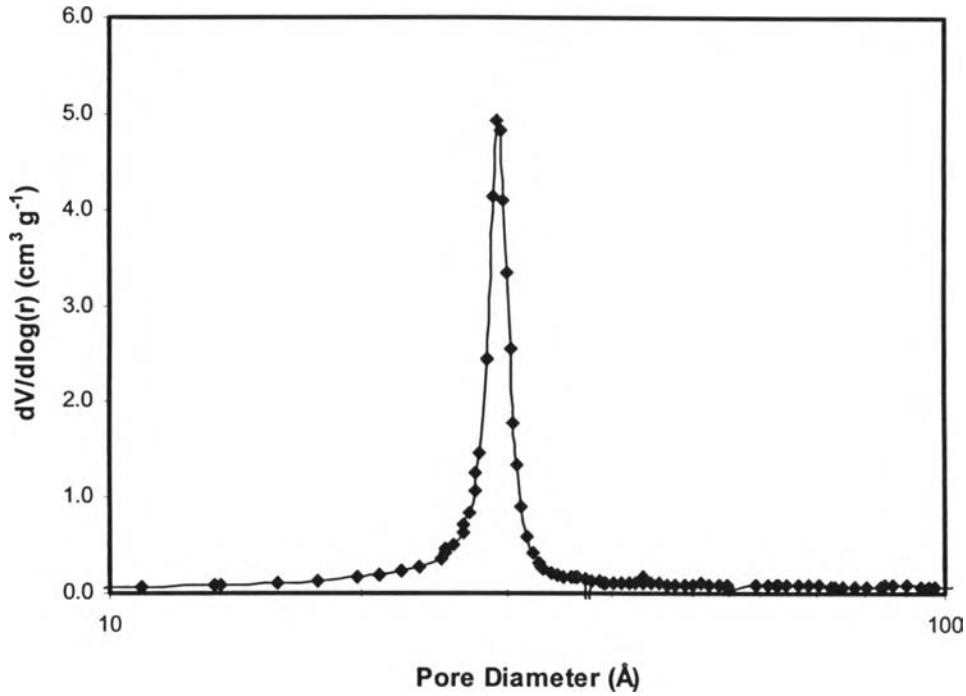

Figure 4-4 Pore size distribution of RH-MCM-41 calculated from nitrogen adsorption isotherms at 77 K using the BJH method.

The comparisons of physical properties obtained from the BET analysis between the synthesized MCM-41 and MCM-41 from references are reported in Table 4-1. It was confirmed that this work gave somewhat similar results to that of others.

Table 4-1 The comparison of physical properties obtained from the BET analysis between the synthesized MCM-41 and MCM-41 from references.

Samples	Pore diameter (Å)	Pore volume ($cm^3\ g^{-1}$)	S_{BET} ($m^2\ g^{-1}$)	Pore wall thickness (Å)
Parent MCM-41*	29.5	0.87	800 ± 25	5.68[a] /6.1[b]
RH-MCM-41**	29.0	0.93	800 ± 8	5.48[a] /5.6[b]
MCM-41***	26.1	0.79	871	6.4
MCM-41****	30.8	0.73	1039	6.2

Remarks:

[a] pore thickness calculated from the BET method.

[b] pore thickness calculated from the method recommended by Naono et al., 1997.

* synthesized by CTAB and TEOS in a basic solution with the aging time of 48 h at room temperature

** synthesized by a CTAB and sodium silicate with an aging time of 48 h at room temperature

*** synthesized by CTAB and TEOS in a basic solution with an aging time of 36 h at 110°C in a Teflon-lined autoclave [Yu et al., 2001].

**** synthesized by CTACl and a sodium silicate in basic solution with an aging time of 16 h at room temperature in a Teflon flask [Naono et al., 1997].

4.3.3.3 SEM and TEM Morphology

The surface morphologies of RH-MCM-41 synthesized within a 48 h aging time and its pH value adjusted at 10 are shown in Figure 4-5. The SEM image in Figure 4-5 (a) indicates the agglomerations of uniformly spherical and drum-like particles with a diameter in the range of 150-200 nm. The TEM image of the hexagonal arrangement with well-defined pore size 2.0-3.0 nm is observed in Figure 4-5 (b). It was seen that the RH-MCM-41 sample performed a unique

characteristic, which is particularly found in mesoporous MCM-41 as reported elsewhere.

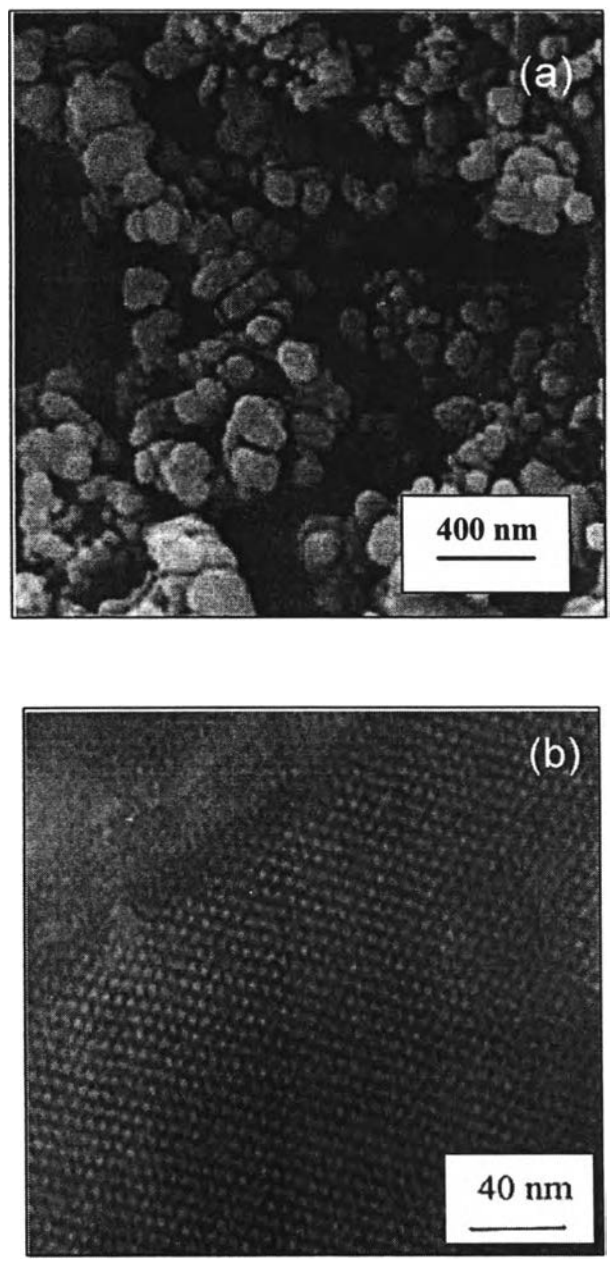

Figure 4-5 SEM (a) and TEM (b) images of RH- MCM-41 with an aging time of 48 h and a pH value of 10.

4.3.3.4 Fourier Transform Infrared Spectrometry (FTIR)

The FTIR spectra of RH-MCM-41 in transmittance mode are shown in Figure 4-6. Similar to the FTIR results of the parent MCM-41 discussed in Chapter III, adsorption peaks identical to siliceous mesoporous solid are observed. The rocking mode near 460 cm^{-1} is due to Si-O bonds. The systematical stretching mode and the asymmetric stretching mode of Si-O-Si are pointed at 800 cm^{-1} and 1080 cm^{-1}, respectively. A broad absorption band around 3470 cm^{-1} is assigned to H-bonded silanols (Si-OH), corporate with the symmetric stretching of Si-OH at 956 cm^{-1}, which is particularly found in MCM-41.

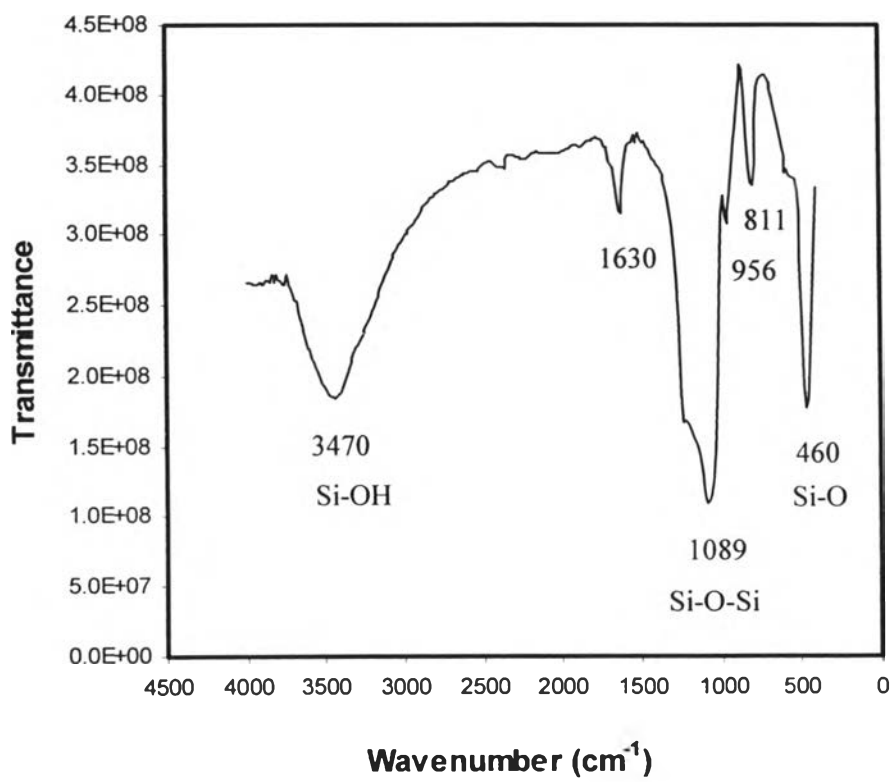

Figure 4-6 FTIR spectra of RH-MCM-41 with an aging time of 48 h and the pH value of 10.

4.4 Adsorption of Chlorinated Volatile Organic Compounds (CVOCs) on RH-MCM-41

4.4.1 Experimental

The adsorption behaviors of CVOCs on RH-MCM-41 were studied by temperature programmed desorption (TPD). A certain amount of pressed RH-MCM-41 pellets was loaded into each studied CVOC solutions (99.8% purity of TCE, PCE, and CT) and kept toward equilibrium time. The experiment was carried out in a 20 ml vial with a Teflon septum and tightly capped with an aluminum lid. MCM-41 was filtered and dried at room temperature before being placed the known amount on a platinum pan and was later analyzed by using thermogravimetric analysis. The weight loss due to desorption at increasing temperature rates set at 3, 5, 12, and 20 $^{o}C\ min^{-1}$ were recorded.

4.4.2 Results and Discussion

Figures 4-7 to 4-9 show the derivative peaks of desorption (-dm/dT) from the TPD of each chemical with different increasing temperature rates. The area under the desorption peak represented the adsorbed amount and the desorption energy was assumed to be close to the adsorption energy.

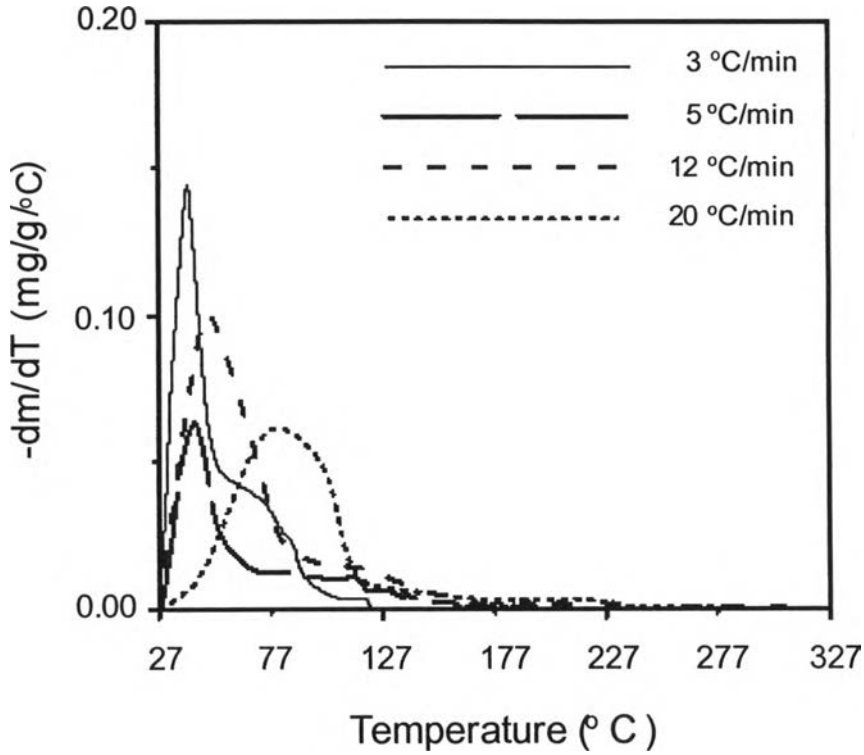

Figure 4-7 TPD profiles of TCE for RH-MCM-41 at different heating rates.

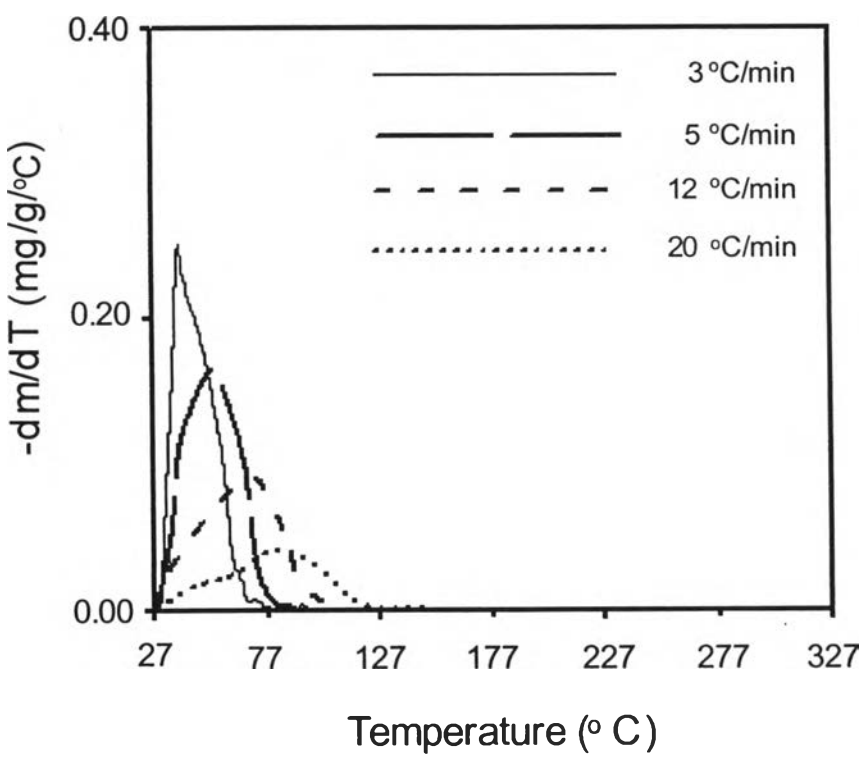

Figure 4-8 TPD profiles of PCE for RH-MCM-41 at different heating rates.

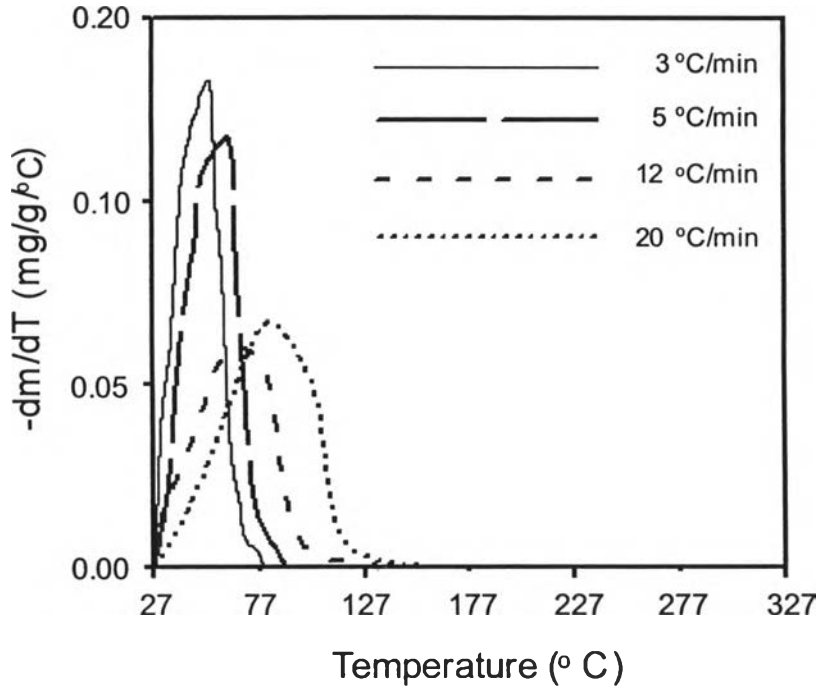

Figure 4-9 TPD profiles of CT for RH-MCM-41 at different heating rates.

The maximum peaks for TCE were shifted from 40 to 43, 49 and 82 °C (Figure 4-7), according to the increasing heating rate. It revealed the chemical desorption from the surface before reaching its boiling point (87 °C). It was found similar to the TPD spectrums of PCE and CT. The maximum peaks for PCE are at 38, 52, 70 and 79 °C (Figure 4-8). Those temperature are lower than its boiling (120 °C). The maximum peaks for CT are 53, 61, 64 and 81 °C (Figure 4-9), which were partially close to its boiling point (77 °C). It was found that for all chemicals, maximum peaks moved to the higher temperatures corresponding to higher increasing temperature rates.

By assuming that the desorption process is first-order and the homogenous surface for adsorption and the readsorption of the desorbed gas does not occur, the desorption energy (E_d) can be calculated from the slope of the plot between the natural log of T_m versus $(T_m)^{-1}$, as shown in the Equation 4-1.

$$2\ln T_m - \ln B = \frac{E_d}{RT_m} + \frac{E_d}{AR} \quad \text{.....(4-1)}$$

Note : T_m is the temperature at the maximum desorption rate, K

E_d is the average activation energy for desorption, J mol^{-1}

B is a heating rate, K min^{-1}

A is the pre-exponential factor

R is the gas constant

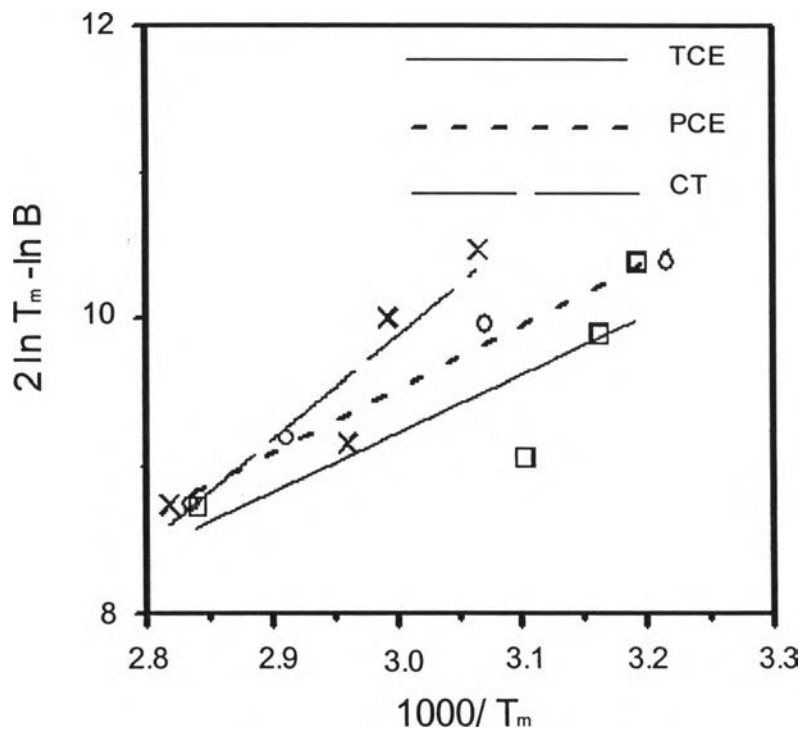

Figure 4-10 Plot of $2\ln T_m$-lnB as a function of $1000/T_m$ over the sample of RH-MCM-41.

The E_d of each TCE, PCE, and CT calculated from Figure 4-10 are 33.2, 35.9, and 58.4 kJ mol^{-1}, respectively. The order of adsorption energy declined from CT, PCE, to TCE. TCE and PCE somewhat adsorbed with moderate adsorption energy, while CT adsorbed more strongly, probably with a covalent bond. These results agree with the to TPD spectrum of those chemicals to MCM-41 as shown in Figure 4-11.

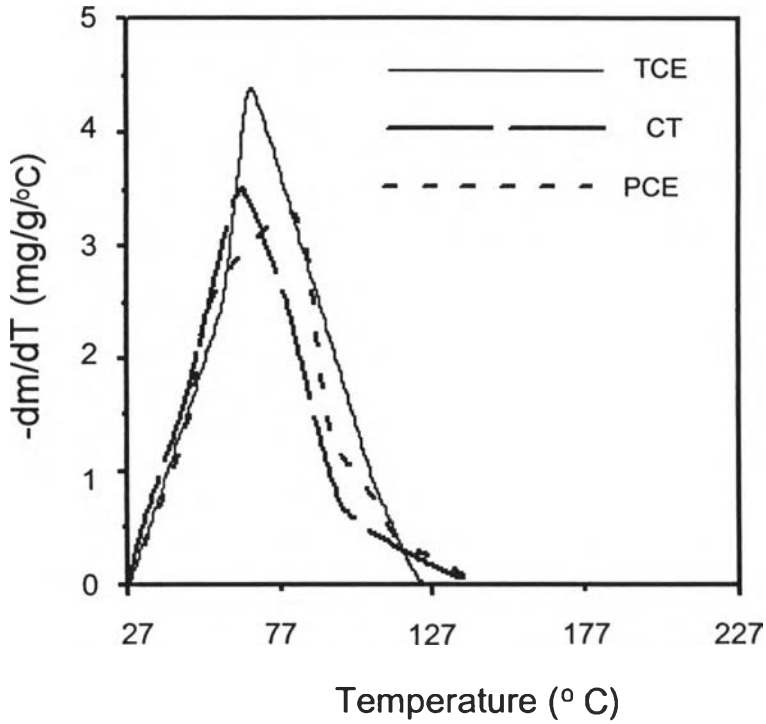

Figure 4-11 TPD profiles of TCE, PCE, and CT over RH-MCM-41 with heating rate of 5 °C min^{-1}.

The TPD of chemicals at a constant heating rate of 5 °C min^{-1} in Figure 4-11 demonstrates that the RH-MCM-41 provided the similar amount of chemical sorption uptake for all three chemicals. It shows that the magnitudes of the sorption uptakes on RH-MCM-41 followed the order of the Henry's law constants: TCE > PCE ~ CT, but slightly different from the order of their boiling points, which was in agreement with Khan et al., 2000.

In addition, the capability for the adsorption of CVOCs of each sorbents were compared with commercial adsorbents including mordenite (ratio of Si/Al = 19) and activated carbon. The properties of commercial adsorbents and RH-MCM-41 are shown in Table 4-2 and the TPD profiles of CVOCs on varied adsorbents are shown in Figures 4-12 to 4-14.

Table 4-2 Properties of commercial adsorbents and RH-MCM-41.

Materials	Surface area (m^2 g^{-1})	Pore diameter (Å)
RH-MCM-41	800	29.5
Activated carbon	1200	6-20*
Mordenite	450	4-18*

Note : * Farrauto et al., 1997.

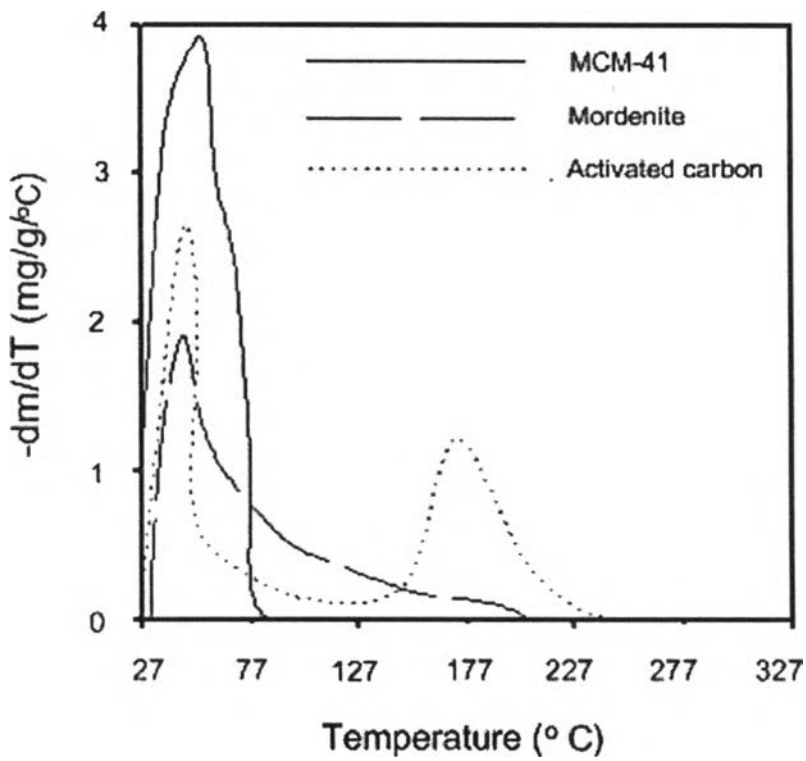

Figure 4-12 TPD profiles of TCE over RH-MCM-41 with a heating rate of 5 °C min^{-1}.

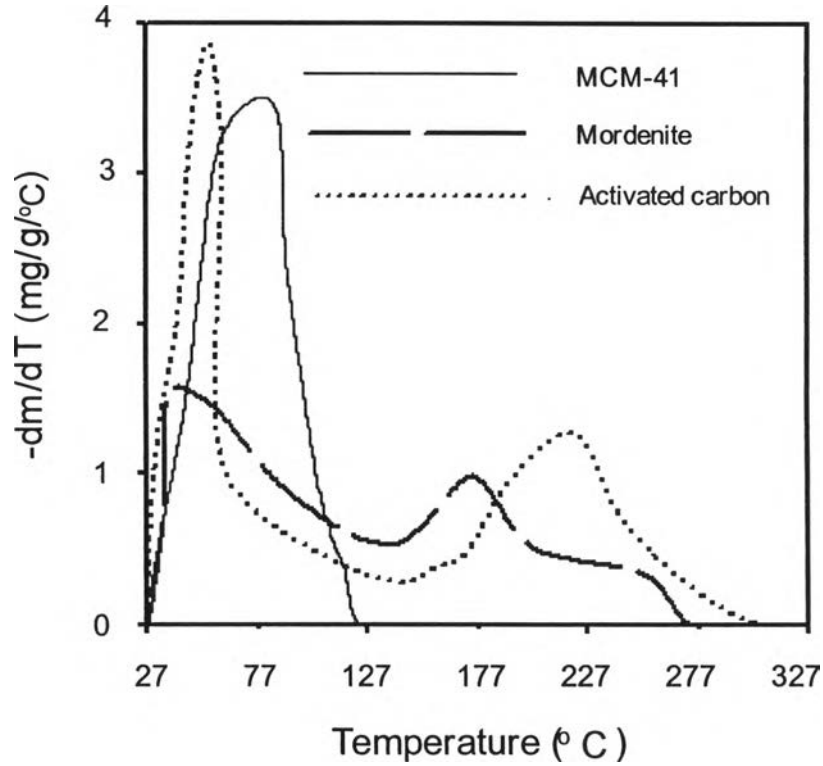

Figure 4-13 TPD profiles of PCE over RH-MCM-41 with a heating rate of 5 °C min^{-1}.

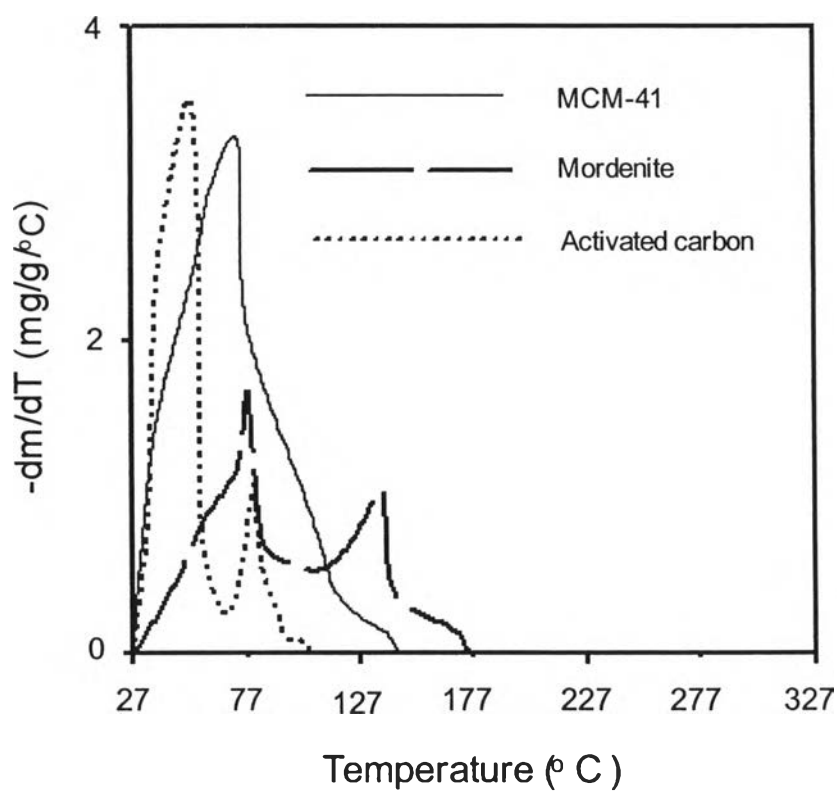

Figure 4-14 TPD profiles of CT over RH-MCM-41 with a heating rate of 5 °C min^{-1}.

Considering the accumulated area under the adsorption peaks, the best adsorption capacity for CVOCs was observed in RH-MCM-41. Moreover, RH-MCM-41 was the only material that adsorbed CVOCs by a single type of active site because RH-MCM-41 possesses a uniform pore size diameter, large enough for CVOCs to adsorb uniformly [Zhao et al., 2000]. One peak at a comparatively low temperature in the desorption profile of RH-MCM-41 suggested self-blocking of the channel network. This information would be useful for further catalytic application. It has been reported that the TPD spectra of organic compounds from microporous zeolite frequently display two-stage desorption processes due to the self-blocking of the channel network by flexible molecules bending through 90^{o} at intersections of the channel system [Richards and Rees, 1986]. Obviously, activated carbon showed two desorption peaks for all tested CVOCs and mordenite showed two peaks for PCE and CT indicating that there are two different active sites or two different pore dimensions. Both mordenite and activated carbon have micropores and mesopores which could be responsible for those two desorption peaks. This result revealed that the high temperature was required for adsorbent regeneration, which might gradually damage surface structure.

4.5 Summary

Highly reactive silica extracted from rice husk can be used for the synthesis of MCM-41 mesoporous molecular sieve. Instead of using TEOS, the well-ordered MCM-41 was satisfactorily obtained from the aqueous mixture of CTAB and sodium silicate utilized from rice husk silica with the molar compositions $1SiO_2$: 1.1NaOH: 0.13CTAB: $0.12H_2O$. The optimum pH value of the synthesis gel was controlled at 10 with an aging time of 48 h at room temperature. The synthesis pH and aging time are significant parameters in the formation of a well-defined mesoporous structure. The optimum pH of the synthesis mixture enhances the degree of polycondensation of the silicate species as well as longer aging time attributes to the well-assembled silicate complex, which eventually provides the formation of uniformly hexagonal crystallites.

Similar to the parent MCM-41, RH-MCM-41 showed the high intensity of the XRD crystallinity peaks and favorable porous characteristics with the nitrogen adsorption isotherm classified as Type IVc. Capillary condensation was found in a very narrow pressure range, indicating the presence of nearly uniform pores in the MCM-41 particles, which agrees very well with the TEM results. The surface area estimated by using the BET method was (800 ± 8) m^2 g^{-1}. The pore size distributions from the nitrogen isotherm using the BJH showed quite narrow pore diameter distributions centered at 29.0 Å. For the adsorption tests, RH-MCM-41 adsorbed a similar amount of TCE, PCE and CT, but the adsorbed CT was stronger than TCE and PCE. RH-MCM-41 had only one kind of active site for adsorption of CVOCs. In contrast, all studied CVOCs adsorbed over two active sites of activated carbon. TCE adsorbed over mordenite on a single site, while PCE and CT adsorbed two active sites. The amount of adsorbed TCE on RH-MCM-41 was greater than that on activated carbon and mordenite. However, PCE and CT adsorbed on RH-MCM-41 as much as activated carbon but more than mordenite.